6. INCREASING THE STABILITY OF THE 3D SCAFFOLDS

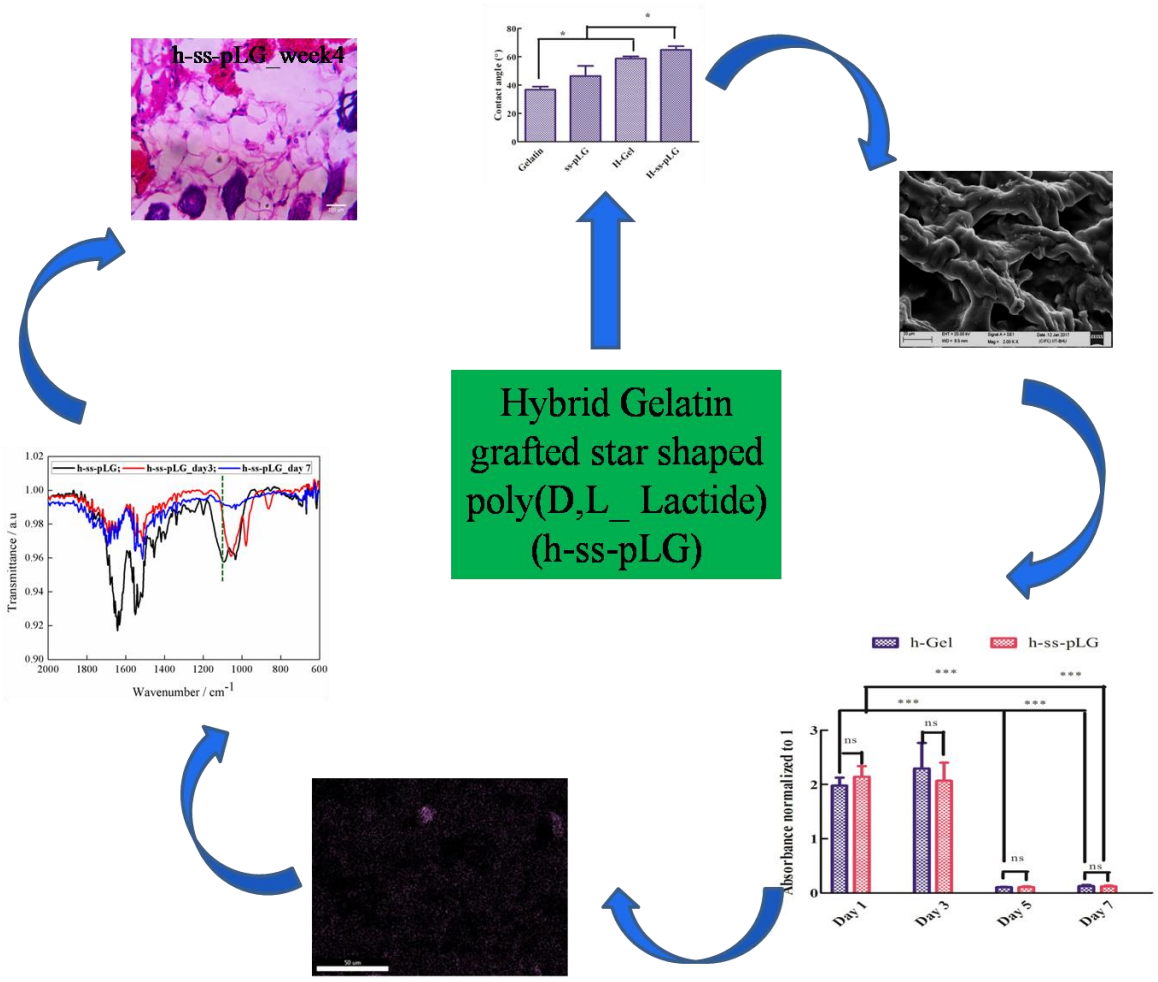

This chapter describes about increasing the stability of scaffolds by covalent cross-linking with glycidoxypropyl trimethoxysilane (GPTMS). The effects of cross-linking in terms of increasing the stability and compatibility is discussed.

6.1. OVERVIEW

Biomaterials based tissue engineering is a popular approach to solve the degeneration of tissue problem, however, biomaterials suitable for tissue engineering must meet some very challenging criteria [177]. For example the scaffold, the template for the tissue growth should exhibit better stability to match the mechanical properties of the host tissue; and resorb with tailored degradation rate.

PLA is a wonderful biomaterial due to its biodegradable nature. The degradation rate and mechanical strength of PLA based 3D scaffolds can be increased by hydroxyapetite [178], bioactive glass [179], cacium phosphate [180]. On the other hand, gelatin is a commercially available biomaterial that is widely used as tissue engineering scaffold due to its biodegradability and similarity to the more expensive collagen adhesive protein. To increase the stability of gelatin scaffolds, various cross-linkers have been used such as glutaldehyde [110], carbodiimide [181], and genipin [182] etc. In addition to that sol–gel derived hybrid materials have also been used, where interpenetrating networks (IPNs) of organic polymers and inorganic components forms biodegradable composite scaffolds [183]. Among the inorganic components, silica-based bioactive glasses are of important class of materials because of the tailored chemical property and controlled degradation when cross-linked with polymers [179].

We have earlier synthesized ss-pLG to make the PDLLA cell adhesive. We also observed the scaffolds fabricated from ss-pLG degraded at faster rate because of the gelatin grafting. The degree of gelatin grafting somehow controlled the degradation rate by linear gelatin grafted poly(D,L-Lactide) (l-pLG) scaffolds but the stability of the scaffolds were not that higher to support cells for longer period. The silica alone is

brittle, further if polymers are introduced to the silica, the resulting hybrid composites with silica will potentially increase the stability and toughness of the materials, which could be particularly used for tissue engineering applications. In that view, γ-glycidoxypropyltrimethoxysilane (GPTMS) was taken as a cross-linker, which is a known silane coupling agent, which consists of epoxy and methoxysilane groups. The epoxy ring of the GPTMS molecules react with the amino or carboxyl groups on the polymeric chain and forms pendent silanol groups (Si-OH) by hydration of the trimethoxy groups on the GPTMS through an acid catalyzed reaction. Further, the condensation process of two Si-OH molecules allows forming Si-O-Si bonds. Thus the cross-linked structures were formed through the Si-O-Si linkages. Therefore, herein we propose to use GPTMS as a cross-linker to hybridize ss-pLG to increase the stability for the tissue engineering application.

In the present study, cross-linking of ss-pLG with GPTMS (h-ss-pLG) and their ability to support cellular proliferation on the hybrid scaffold is demonstrated. The covalent cross-linking will increase the hydrophobicity and thus the stability of the matrix. In accordance to assess our hypothesis, we studied contact angle and followed by culturing Hep-G2 cells within the h-ss-pLG scaffolds. On the other hand, we also prepared gelatin cross-linked scaffolds (h-Gel) for the comparative study.

6.2. RESULTS AND DISCUSSION

6.2.1. Synthesis and characterization of hybrid gels

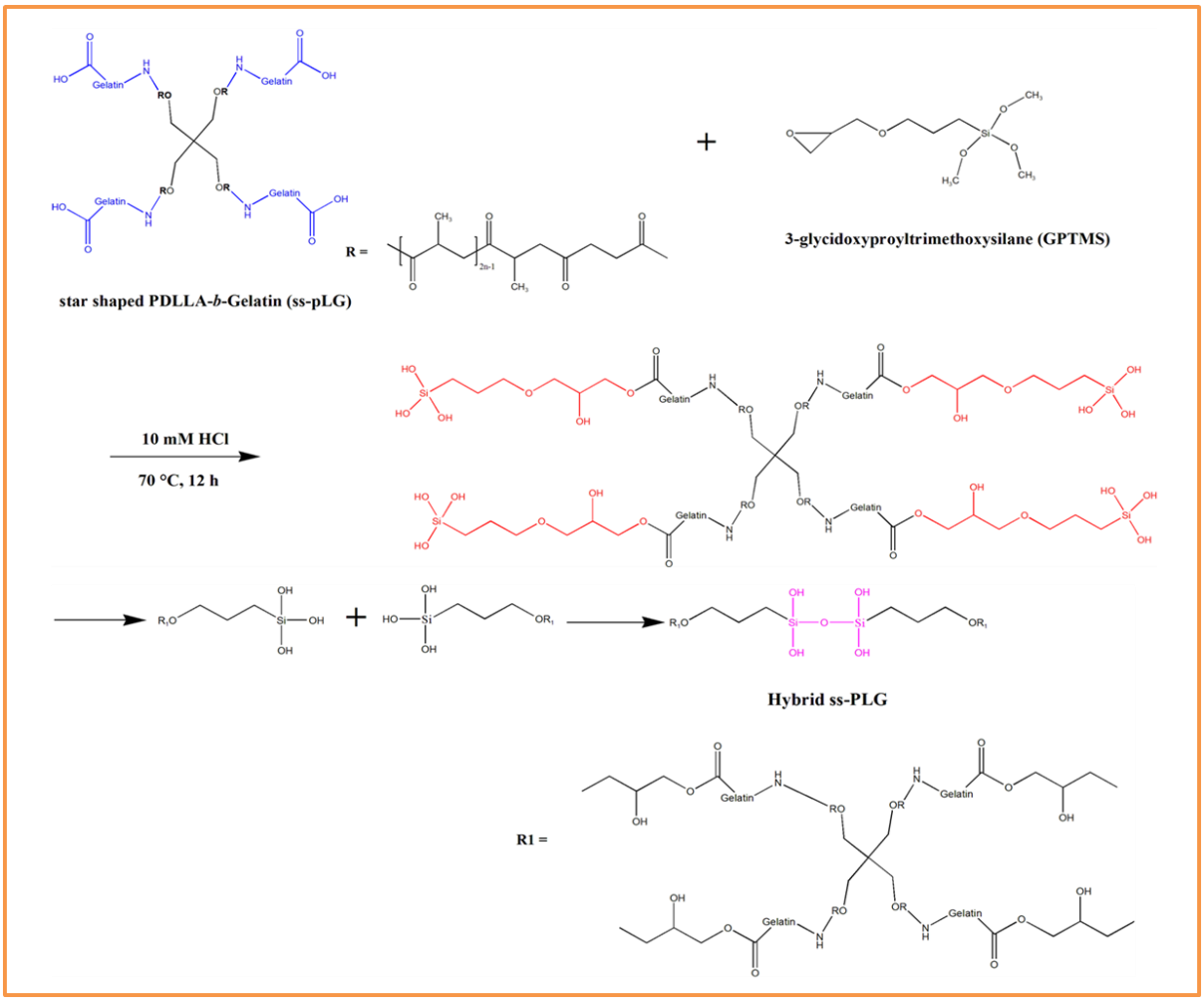

Figure 6.1. Reaction scheme for the synthesis of silane cross-linked gelatin grafted star shaped PDLLA(h-ss-pLG)

Figure 6.1 represents the synthesis of hybrid silica cross-linked gelatin grafted star shaped PDLLA (h-ss-pLG) using GPTMS. The synthesized hybrid gels h-Gel and h-ss-pLG was characterized initially by using FTIR. **Figure 6.2** shows the FTIR spectra of hybrid gels, in the wave number range of 600 to 4000 cm^{-1}. The unmodified Gel and ss-pLG polymer was also characterized to compare it with the synthesized silica cross-

linked hybrid polymers. The Si–OH band at 910 cm^{-1} which was almost disappeared and Si-O-Si band at 1115 cm^{-1} was broadened for the hybrid Gels (**Figure 6.2**A, B),

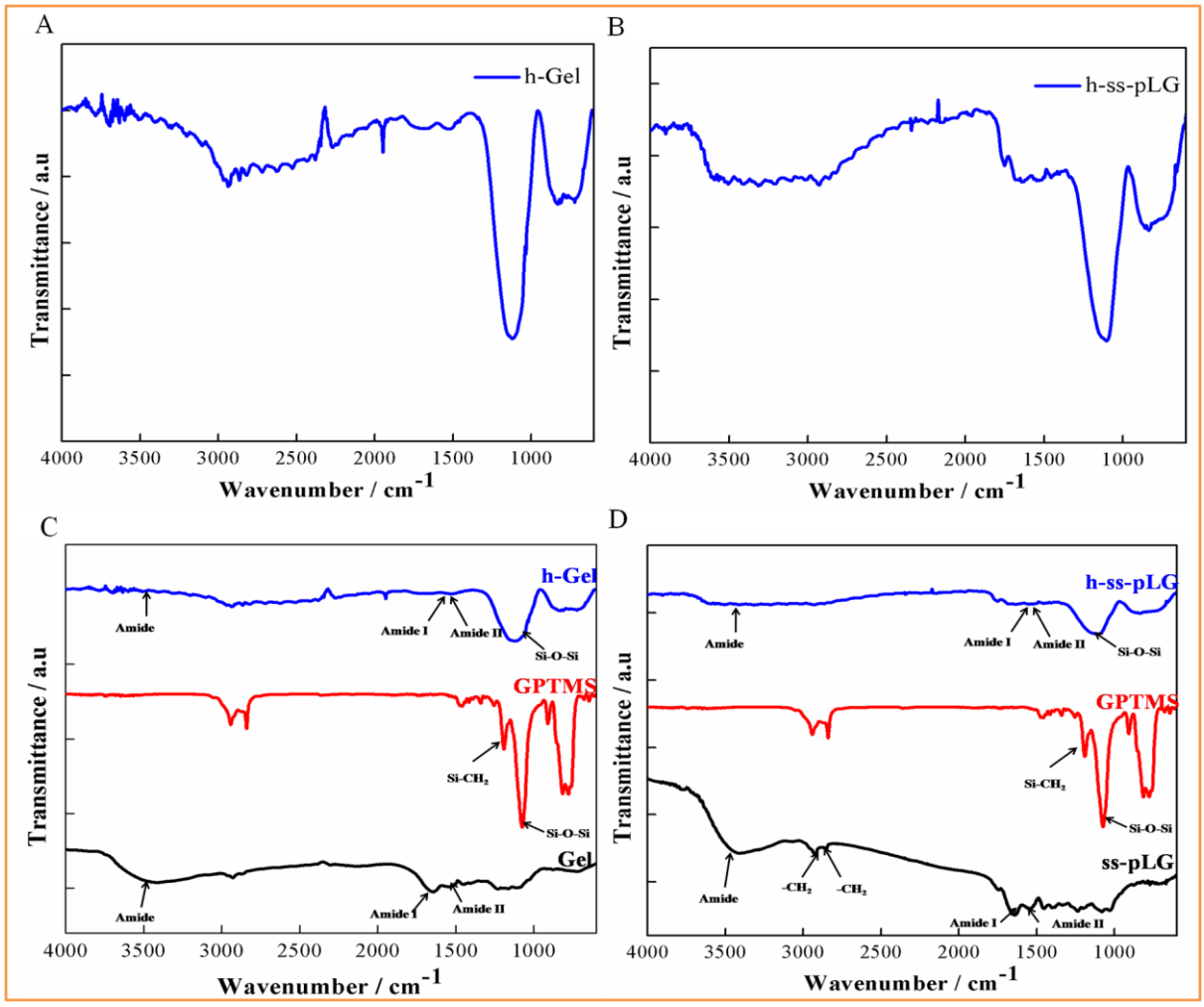

Figure 6.2. Characterization of hybrid gels. FTIR spectra of (A,C) silane cross-linked gelatin (h-Gel) and (B,D) silane cross linked ss-pLG (h-pLG)

suggesting that a more highly condensed interpenetrating silica network formed. The Gel and ss-pLG showed the characteristic peaks at 1661 and 1688 cm^{-1} for its distinct C=O bond vibration, respectively [106, 184]. After cross-linking of GPTMS with Gel and ss-pLG the C=O stretching peaks shifted to lower frequencies at 1642 and 1627

cm^{-1}. This clearly indicates that strong covalent coupling occurred between Gel, ss-pLG and GPTMS.

6.2.1.1. Thermal properties of hybrid gels

Figure 6.3 shows the thermal properties of Gel, h-Gel, ss-pLG and h-ss-pLG. The thermogravimetric analysis (TGA) of unmodified and hybrid gels are presented in **Figure 6.3**A. Thermal degradation profile of unmodified and hybrid gels were quite different. It can be seen that unmodified polymers Gel and ss-pLG showed T_{onset} at 225 and 209 °C whereas T_{max} of the polymers were found to be 457 and 455 °C respectively(**Table 6.1**). On the other hand, the modified hybrid gels of h-Gel and h-ss-pLG showed improved thermal properties than their original unmodified polymers, where T_{max} was found as 495 °C and 504 °C, respectively. (**Figure 6.3**A). This thermal behaviour may be attributed due to the strong covalent binding of GPTMS with the respective polymer and it is evident that the h-Gel and h-ss-pLG have better thermal stability than their countered unmodified polymers.

Table 6.1 Thermal degradation properties of Gel, ss-pLG, and h-Gel, h-ss-pLG determined by TGA

S.No	Sample(s)	T_{onset} (°C)	T_{max} (°C)
1.	Gel	225	457
2.	ss-pLG	209	455
3.	h-Gel	311	495
4.	h-ss-pLG	326	504

DSC thermograms of Gel, ss-pLG and modified h-Gel, h-s-pLG are shown in **Figure 6.3**B. T_gs of Gel, ss-pLG, h-Gel and h-ss-pLG were observed at 142.9, 112.59 114.87 and 126.46 °C, respectively. The shifting of T_g clearly says the cross-linking was done successfully. On the other hand, T_g of h-Gel was reduced from its countered unmodified Gel, which could be due to the self assembly of the molecules and condensation of water molecule from them. The condensation will lead to reduce in the molecular weight.

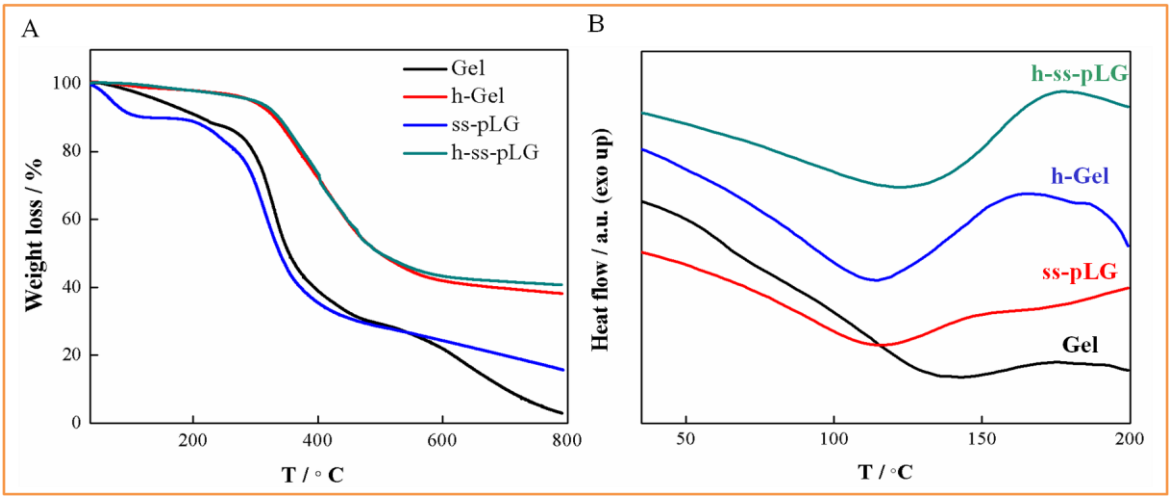

Figure 6.3. Thermal Properties of hybrid gels. (A) TGA thermograms of linear unmodified and gelatin grafted polymers. (B) DSC thermograms of linear unmodified and gelatin grafted polymers.

6.2.2. Cell spreading on 2D hybrid polymer coated film

The surface hydrophobicity is a key factor which governs the cell response. Water contact angle was used to characterize the hydrophilicity of the newly synthesized h-Gel and h-ss-pLG. The contact angle measurement indicate that unmodified gelatin and

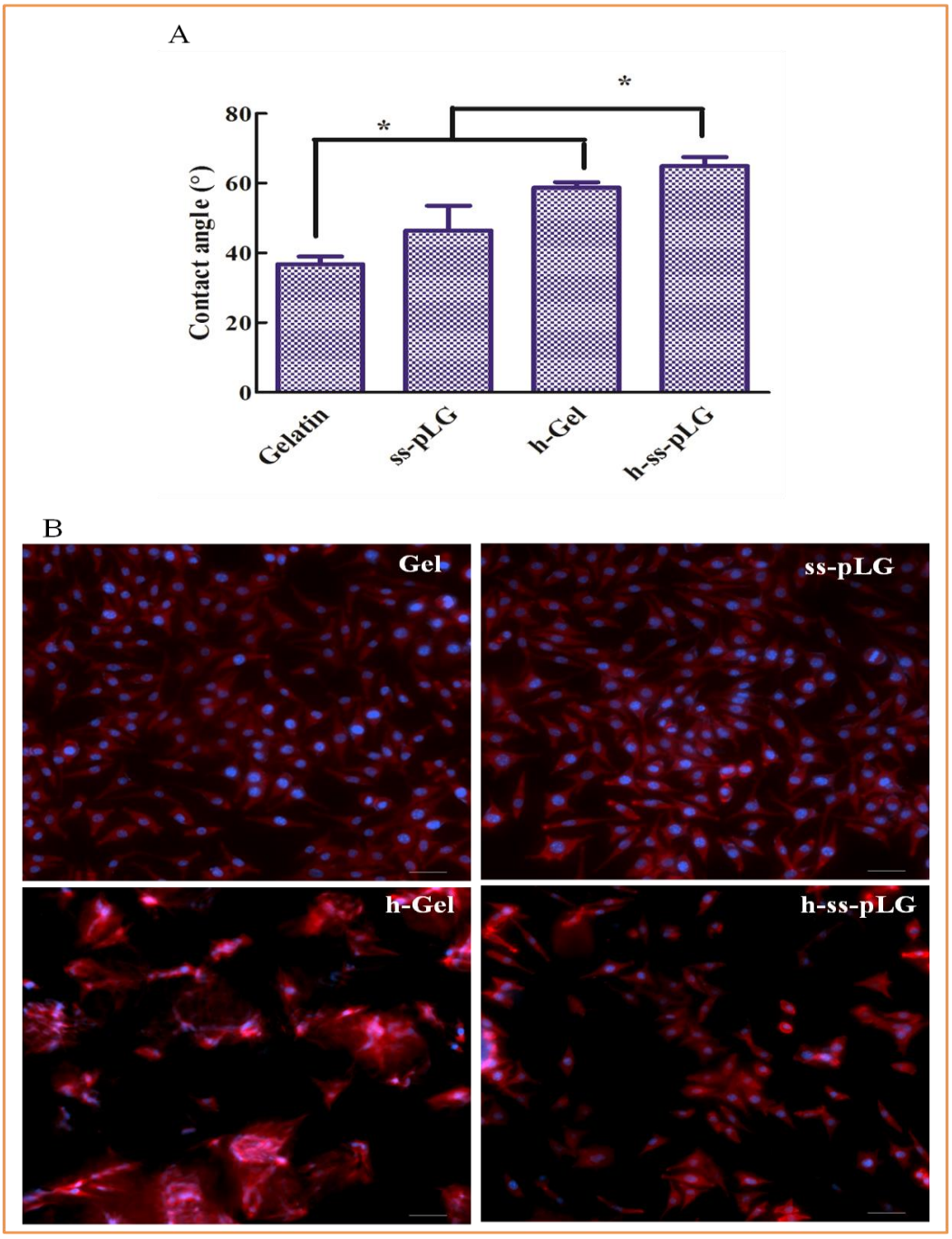

Figure 6.4. Demonstration of cell spreading behavior on hybrid polymer coated 2D cover glass; (A) Contact angle measurements of unmodified and hybrid polymer coated 2D cover glass. (B) Fluorescent colocalized images of F-actin integrated with nucleus shows the spreading of 3T3 cells over the hybrid polymer coated 2D cover glass compared to that of unmodified polymers, after 48 h of culturing. Blue shows the cell nuclei; Red shows the actin filament

ss-pLG were more hydrophilic than the hybrid h-Gel and h-ss-pLG (**Figure 6.4**A). The higher hydrophobicity of h-ss-pLG than h-Gel could be attributed to the efficient cross-linking of GPTMS with ss-pLG and Gel.

Further, we examined the cellular proliferation ability of 3T3 cells cultured (2D) on h-Gel and h-ss-pLG by fluorescent imaging technique. The F-actin filament of the 3T3 cells were probed by Rhodamine Phalloidin red-orange fluorescent dye and the nucleus were counterstained using DAPI (**Figure 6.4**B). The image indicates that the spreading of cells were not that well supported on hybrid polymer coated coverglass, whereas it facilitated small spheroid like structures, which was due to the hydrophobicity of hybrid polymers.

6.2.3. Fabrication and Characterization of scaffolds

The hybrid gels were frozen and freeze dried to get porous scaffolds. The structural complexity of tissue engineering scaffolds should be similar to native tissue in-order to suit the intended biological function [185]. Biological tissues generally have a gradient porous structure where porosity is not uniform. Rather, the natural engineering of porous architecture will be in such a way to maximize the overall performance of the structure. For instance, scaffolds employed in angiogenesis process (regeneration of a blood vessel/vascularization) should have the pores with a diameter of 20 to 40 μm in-order to enable the exchange of metabolic components and to facilitate endothelial cell entrance[186]. Even though, higher pore sizes and porosity may facilitate nutrient, oxygen delivery and can enable more cell growth, the large amount of void volume may mitigate the mechanical properties of the scaffold[187].

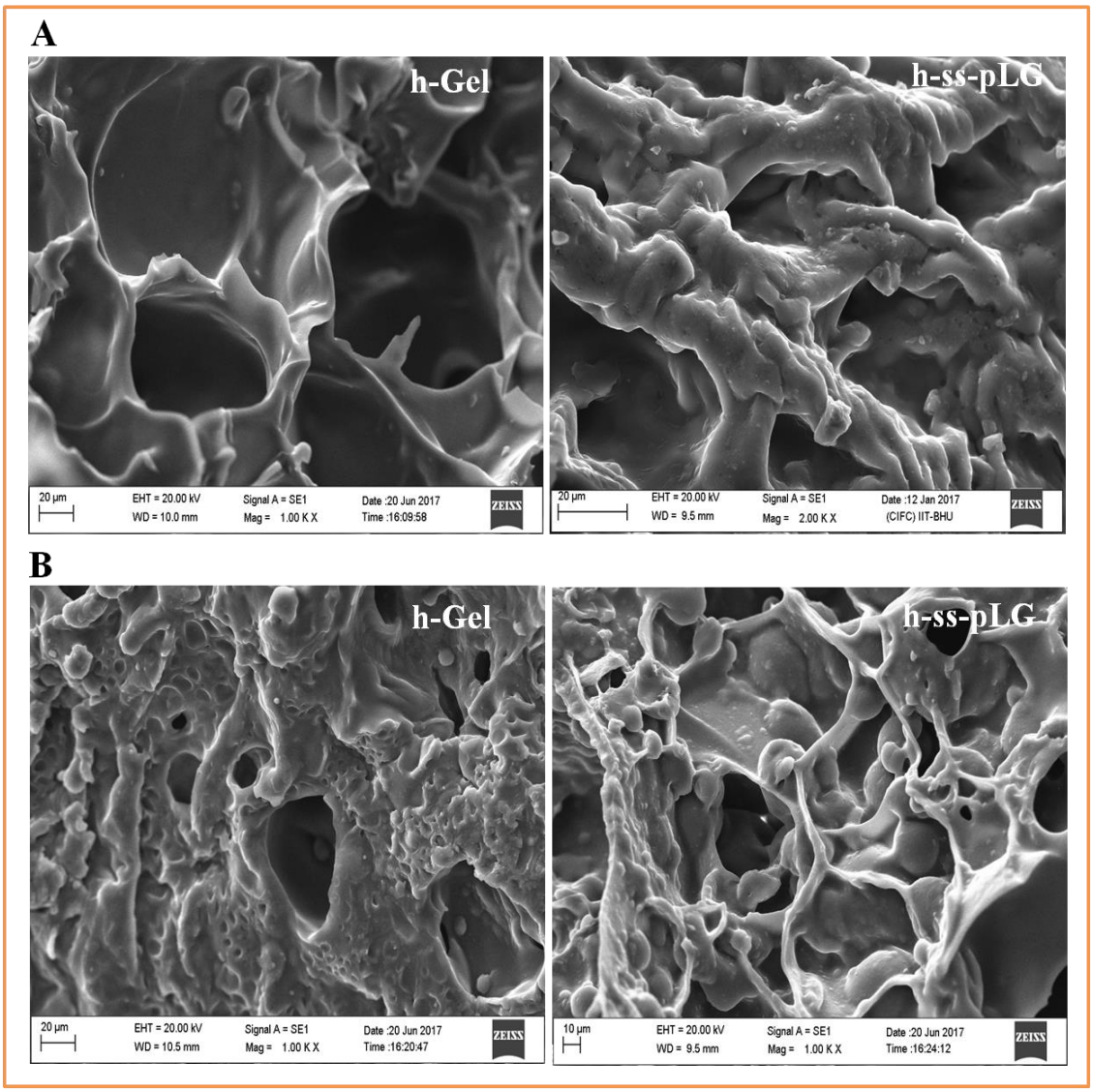

Figure 6.5. Surface morphology of hybrid scaffolds analysed by SEM. (A) The fabricated hybrid scaffolds. (B) 3T3 cells seeded scaffolds after 3 days of culturing.

We used scanning electron microscopy (SEM) to gain qualitative surface morphology information about the molecular architecture of newly fabricated h-Gel and h-ss-pLG scaffolds. **Figure 6.5**A shows the SEM image of h-Gel and h-ss-pLG respectively. h-Gel displayed a distorted elliptical porous architecture with pore sizes approximately ranging between 35±12 µm. However it is to be noted that the not all the pores are of uniform size pore sizes were in the range from 20 µm to 50 µm. On contrary, the

resulting h-ss-pLG 3D scaffolds showed thicker walls of 3D morphology and pore sizes were of 40±8 μm. Apparently, cross-linking ss-pLG showed higher pore size compared to h-Gel which could be due to the branched structure.

Further, SEM images of 3T3 cells seeded scaffolds were acquired to check the cellular growth behaviour within 3D scaffolds. We observed the thick wall of h-ss-pLG became thinner and better cell growth was appeared in h-ss-pLG compared to h-Gel (Figure **6.5**B)

6.2.4. Cell proliferation within hybrid scaffolds

In order to examine the cellular compatibility of the hybridized h-Gel and h-ss-PLG we studied the cell proliferation, *in vitro*, by assessing the cell metabolic activity using 3-(4,5-dimethylthiazol-2-yl)-2,5-diphenyltetrazolium bromide) (MTT). The absorbance rates of the h-Gel and h-ss-PLG were lower than the unmodified Gel and ss-pLG after 3 days of culturing (**Figure 6.6**A), this indicates a reduction in the rate of cell proliferation and reduction in overall cell viability. To investigate the factor that affect the cell proliferation, we performed the MTT assay to study the cytotoxicity for various concentration of (0.1 - 2%) of GPTMS, which was the additional component involved to make the hybrid gel. Increasing concentration of GPTMS induces cytotoxicity in concentration dependent manner (**Figure 6.6**B). However, 2% GPTMS showed less than 6% cytotoxicity which is within the accepted range (10%). Therefore it is clear that GPTMS play less significant role in inducing the cytotoxicity.

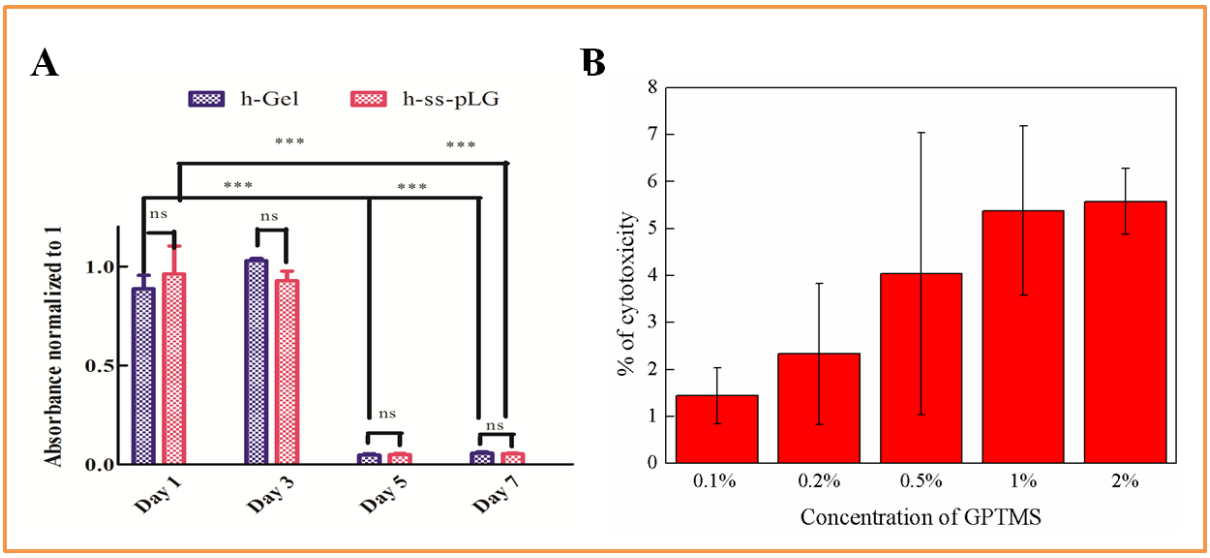

Figure 6.6. Demonstration of rate of cell proliferation within the hybrid scaffolds (A) Cell Proliferation of Hep-G2 within the scaffolds assessed by MTT assay, cell number was related to 1 according to the growth of cells on 2D culture plates at day 3. All bars expressed as mean values ± SD (n=3); * p <0.05 , **p<0.001 *** p<0.0001. (B) Cytotoxicity of GPTMS at various concentration against Hep-G2.

6.2.5. Silica release

In the previous study, we observed decrease in the rate of cell proliferation in silane cross-linked hybrid scaffolds (h-Gel and h-ss-pLG). However, the reason for the reduction in cellular proliferation stand unaddressed owing to less significant effect of GPTMS on cytotoxicity against Hep-G2 cells. It is our hypothesis that the release of silica from the h-Gel and h-ss-pLG could be the reason, which reduces cell proliferation, *in vitro* since it has been reported that silica material possess good cell adhesion property. In order to validate our hypothesis, we quantified the initial silica level (%silica) present in the system. We assessed the silica level after day 3 and day 7 (post cell culture media incubation) by energy dispersive X-Ray analyzer (EDX). Interestingly we observed the reduction in the silica profile of the scaffold.

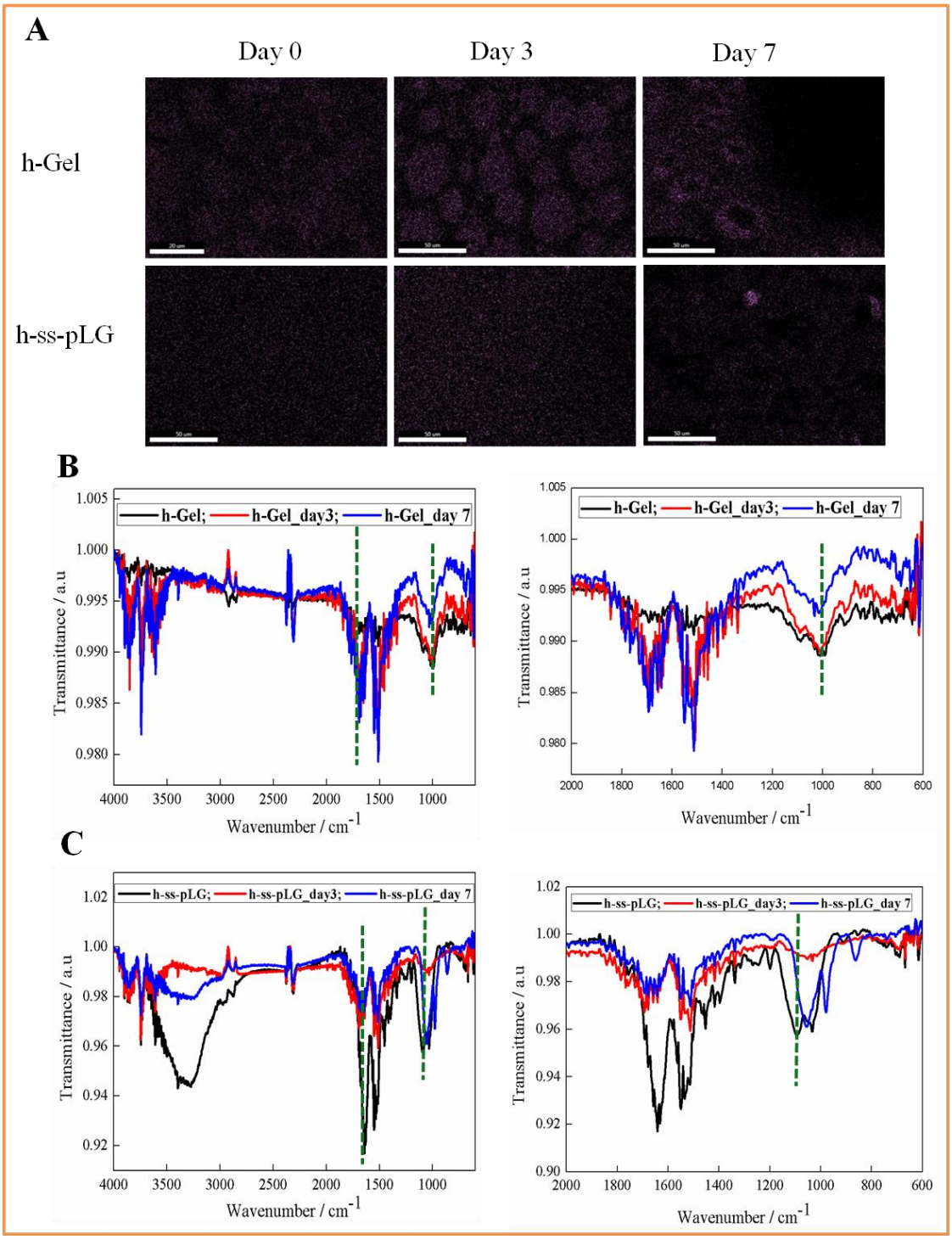

Figure 6.7. Qualitative release kinetics of silica from hybrid scaffolds (A) Elemental mapping and (B,C) FTIR of hybrid scaffolds before and after incubating in cell culture media

Figure 6.7A shows the silica release profile at day 0, 3 and 7 observed by elemental mapping through EDX for the h-Gel and h-ss-pLG samples. We could clearly see the decrease in the intensity of silica element after day 3 and 7 of incubation in the cell culture media. The silica quantity (%silica) in h-Gel at Day 3 (20.58±3.27) was lower than the initial silica level at day 0 (22.81±3.11), this was further reduced to 15.95±3.37 on day 7. Similarly, the %silica in h-ss-pLG at day 7 (14.83±3.72) was much lower than the %silica at day 0 (18.27±5.94) and day 3 (15.3±3.84) (**Table 6.2**). The significant level of silica released from the scaffold to cell culture medium observed by EDX provides a strong evidence to validate our hypothesis. Furthermore, we studied the silica release profile in h-Gel and h-ss-pLG by FTIR after day 3 and day 7. We observed the Si-O-Si in phase stretching band around 1115 cm^{-1}. The decrease in the Si-O-Si band stretching indicates release of silica with time **(Figure 6.7**B**)**.

Table 6.2. Quantitative release kinetics of silica from hybrid scaffolds assessed by EDX analysis

Sample(s)	**Day 0**	**After incubation in cell culture media**	
		Day 3	**Day 7**
h-Gel	22.81±3.11	20.58±3.27	15.95±3.37
h-ss-pLG	18.27±5.94	15.3±3.84	14.83±3.72

6.2.6. Hemocompatibility

Furthermore, we studied the hemocompatability of the h-Gel and h-ss-pLG in human blood, *in vitro*. Normally platelets do not adhere to endothelial cells in the circulating blood. However, blood when exposed to foreign surface the platelets tend to deposit and form a layer of proteins and cells, that is followed by immune system activation and initiation of coagulation process. The hemolysis was studied, *in vitro*, h-Gel and h-ss-pLG shown no significant difference in the when compared to their respective unmodified counterparts after 1h and 8h **(Figure 6.8**A**)**. However, the hemolysis was high for h- Gel and h-ss-PLG, at both 1h and 8h, which could be due to the hydrophobicity of the hybrid scaffols.

Similarly, we evaluated the membrane integrity of erythrocytes when incubated with scaffolds by quantifying the enzyme LDH. At different time point, the possible change in membrane integrity of erythrocytes by the scaffolds was observed. The unmodified scaffolds (ss-PDLLA and ss-pLG) incubated with erythrocytes did not show any significant increase, whereas significant increase in release of LDH was observed when incubated with hybrid scaffolds ($p>0.05$) in LDH release when compared to PBS (negative control) after 1 h and 8 h interval, which could be attributed to the hydrophobicity of hybrid scaffolds (**Figure 6.8**B). These results indicate that the hybrid scaffolds induce small disturbance in the membrane integrity of erythrocytes.

Figure 6.8C present the photomicrograph of SEM image displaying negligible number of damaged RBCs when incubated with both h-Gel and h-ss-pLG. The qualitative imaging results comply with our quantitative hemolysis and LDH release.

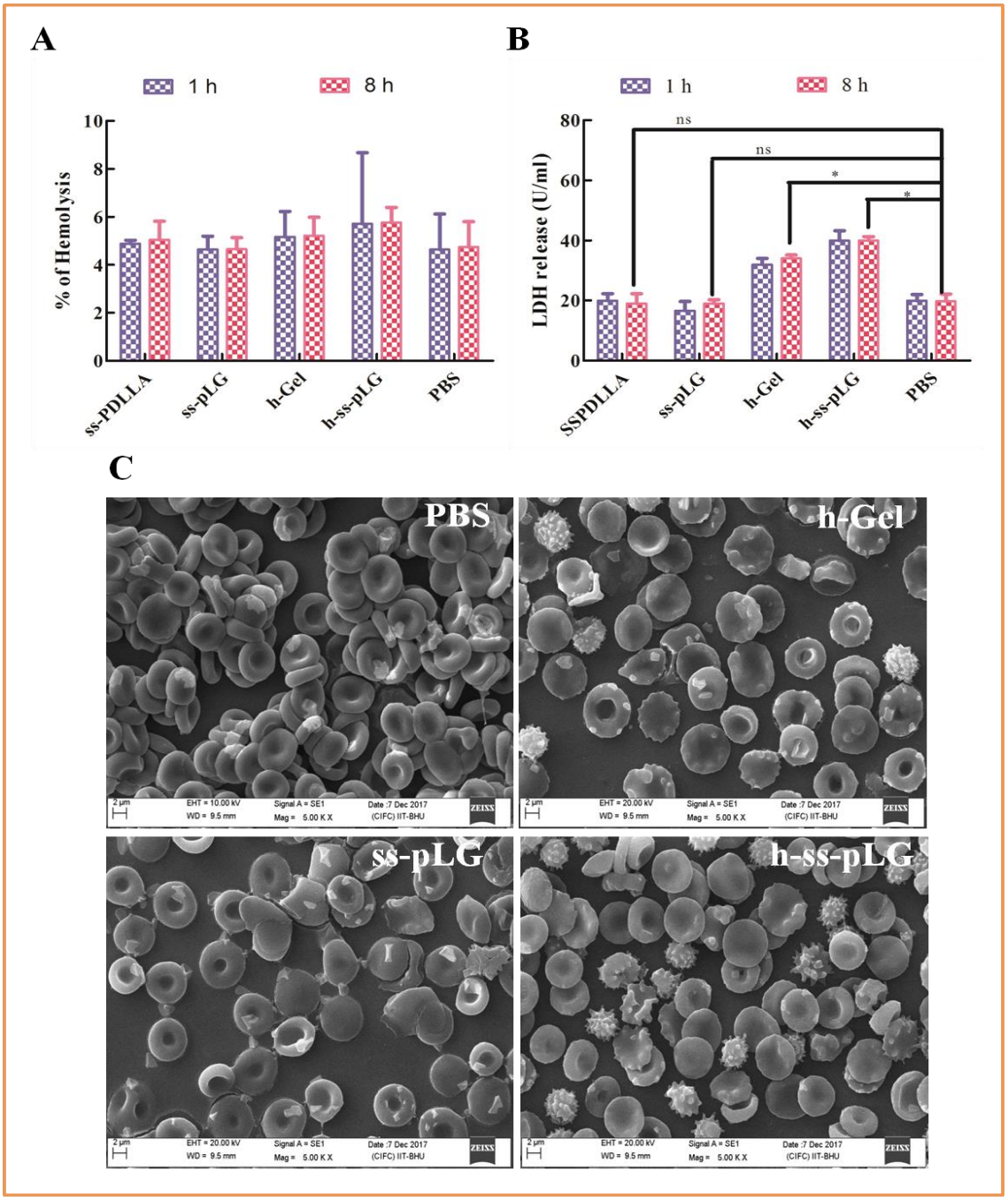

Figure 6.8. Hemocompatability of hybrid scaffolds compared to its counter part (A) Hemolysis of the scaffolds after 1 h and 8 h, no significant difference were observed in comparison to that of PBS; (B) Erythrocytes membrane integrity in presence of scaffolds by LDH release assay. (C) Morphology of RBCs after 4 h incubation with hybrid scaffolds

Therefore, we concluded that the silane cross-linking have less significant effect on the hemcompatability when compared with their unmodified counterparts.

6.2.7. Subcutaneous implantation of implantation of scaffolds and immune response

In vivo experiments were conducted to evaluate the host immune response, implant integration, and immunoisolation behavior of the scaffolds. We investigated the biodegradation and tissue biocompatibility of unmodified and hybrid acellular scaffolds after subcutaneous implantation in rat. After 1 and 4 weeks post implantation, we

Table 6.3. Weight loss profile of the Rats after subcutaneous implantation of scaffolds

Sample(s)	**Weight(g)**		
	Initial	**Week 1**	**Week 4**
Control	200±6	206±8	222±7
Sam	200±8	197±5	204±12
Gel	200±4	192±6	204±9
ss-PDLLA	200±5	194±10	208±4
ss-pLG	200±3	189±8	203±13
h-Gel	200±7	183±7	197±9
h-ss-pLG	200±3	178±8	192±11

retrieved the scaffolds from the implanted site with the overlying native tissues and performed histological examination to assess the infiltration of inflammatory cells. The incision lead to loss in the weight of the animals and animals were gaining weight slowly. The rate of weight gain was relatively good compared to the Sam group (**Table 6.3**). **Figure 6.9** presents the photomicrographs of the H&E stained tissues at the implant site.

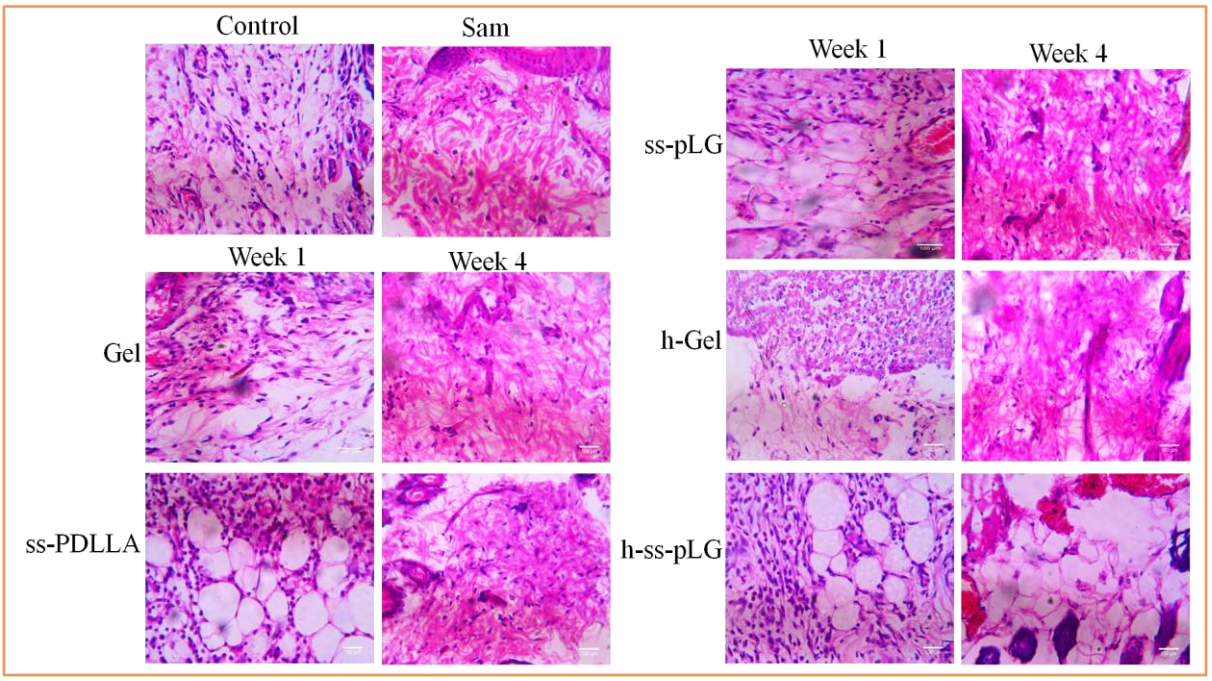

Figure 6.9. *In vivo* compatibility of hybrid scaffolds. H&E staining of retrieved acellular unmodified and hybrid scaffolds after 1 and 4 weeks of subcutaneous implantation in female rat.

We observed minimal inflammatory cells (granulocytes) accumulated at the implant sites in the H&E images (**Figure 6.9**). In addition, higher cell infiltration and cell attachment was observed after week 1 in all the tested scaffolds. The unmodified Gel, ss-PDLLA and ss-pLG scaffolds were completely degraded after week 4, the excised tissue were comparatively looking like the control tissue, which indicates the degraded

product or the scaffold was not affecting the tissue. On the other hand, the hybrid scaffolds h-Gel and ss-pLG were not degraded as they were cross-linked with silane and little infiltration of cells were observed. The results from the animal study demonstrated that unmodified and hybrid scaffolds have good tissue compatibility and also facilitate cell infiltration.

6.3. Conclusion

In this work, we report the hybrid scaffolds fabricated from ss-pLG and Gel which are cross-linked with GPTMS. The cross-linking of silane with ss-pLG and Gel significantly increased the hydrophobicity of the hybrid polymer. The cell proliferation evaluation within the hybrid scaffolds showed after day 3, there was a drastic decrease. The decrease in the cell proliferation could be attributed to the release of silane from the matrix and the cross-linker GPTMS alone was not showing any cytotoxicity against Hep-G2. Therefore, we hypothize that the cells adhered onto the matrix also coming out when the silane is leached out from the matrix. The *in vivo* subcutaneous implantation study showed that Gel, ss-PDLLA and ss-pLG scaffolds degraded completely after week 4, wheras the hybrid scaffolds h-ss-pLG and h-Gel were not degraded as they were cross-linked with silane. The histology analysis showed higher infiltration of cells and the healthy morphology of cells and nucleus was observed in all scaffolds after week 1. On the other hand, the infiltration of cells was lower in hybrid scaffolds after week 4.